Low-frequency wave-energy amplification in graded two-dimensional resonator arrays

Malte A. Peter

Institute of Mathematics
University of Augsburg, Germany

Joint work with L. G. Bennetts (Adelaide) and R. V. Craster (Imperial College).

October 07th, 2019

Motivation

Wave-energy converters in the ocean suffer from low efficiency.

Idea

Use structure(s) in the ocean to amplify the ocean-wave amplitude at power take-off site.

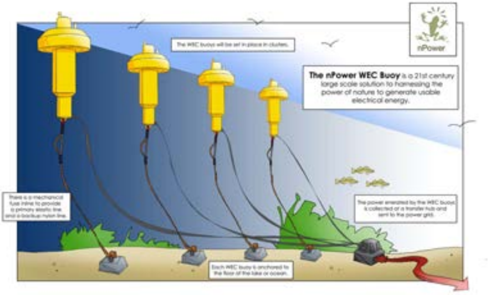

source: zd.net

Motivation: Superlensing of water waves

In standard wave refraction, the directions of the incident and refracted waves lie on different sides of the normal direction of the interface between two media.

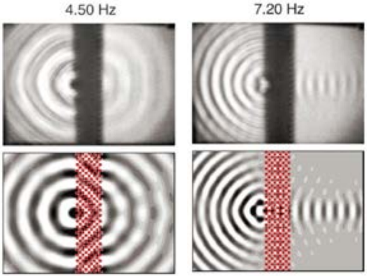

Hu et al. (2004)

$\rightsquigarrow$ *metamaterials* with periodic structure.
Further investigations by Li & Mei (2007) and Farhat et al. (2010).

Motivation

Periodic arrangements of bodies significantly influence the propagation properties of waves compared to the open ocean. E.g. pass bands and stop gaps exist and the group velocity depends on the structure.

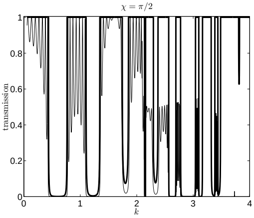

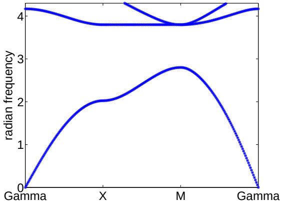

Motivation

Periodic arrangements of bodies significantly influence the propagation properties of waves compared to the open ocean. E.g. pass bands and stop gaps exist and the group velocity depends on the structure.

Idea

Create structure with slowly modulated properties (e.g. spacing) to slow down the waves and, thereby, focus the wave energy.

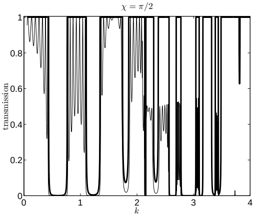

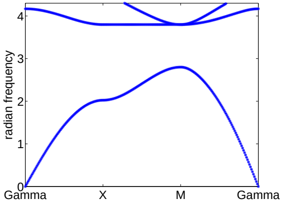

(Idea is based on ideas of Romero-Garcia et al., 2013, for an acoustics problem)

At the last workshop in Herrsching ...

(a) Chirp spacing in 2d arrays of full cylinders

At the last workshop in Herrsching . . .

(a) Chirp spacing in 2d arrays of full cylinders

(b) Chirp radius in single-line arrays of C-shaped cylinders

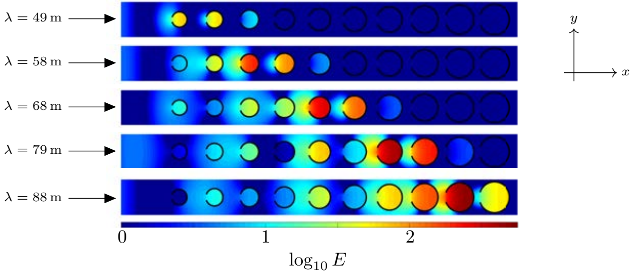

Mathematical formulation

Use linearised inviscid theory, consider irrotational motion and fixed radian frequencies ω only. $\rightarrow \Phi(\mathbf{x}, t) = \mathbb{R}\mathrm{e}\{\phi(\mathbf{x})\mathrm{e}^{-\mathrm{i}\omega t}\}$.

Writing $\alpha = \omega^2/g$, for water of constant finite depth d, the velocity potential ϕ has to satisfy the standard boundary-value problem,

$$
\begin{aligned}
\nabla^2\phi &= 0, && \mathbf{x} \in D, \\
\partial_z\phi &= \alpha\phi, && \mathbf{x} \in \Gamma^{\mathrm{f}}, \\
\partial_z\phi &= 0, && \mathbf{x} \in D,\ z = -d,
\end{aligned}
$$

where D is the domain occupied by the water and Γ^{f} is the free water surface assumed at $z = 0$. At the immersed body surface Γ_j of body Δ_j,

$$
\partial_n\phi = \mathbf{v}_j, \qquad \mathbf{x} \in \Gamma_j,
$$

where $\mathbf{v}_j$ is the normal velocity of the body supplemented by the equations of motion for the body.

$+$ boundary conditions away from the body.

Bloch waves

Let $R\mathbf{i}$ and $S\mathbf{j}$ be two (two-dimensional) vectors that span the rectangular lattice: that is every translation between the mean-centre position of bodies in the horizontal plane has the form of a *lattice vector*

$$\mathbf{R} = m_1 R\mathbf{i} + m_2 S\mathbf{j},$$

where $m_1, m_2 \in \mathbb{Z}$. The corresponding *reciprocal lattice vectors* $\mathbf{K}$ satisfy

$$\mathbf{K} \cdot \mathbf{R} = 2\pi p,$$

where $p \in \mathbb{Z}$.

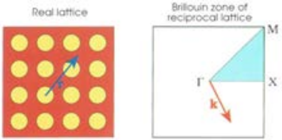

(picture taken from Joannopoulos et al., 1995)

Bloch waves

Periodicity of the geometry motivates to look for periodic solutions satisfying

$$\phi(\mathbf{y} + (\mathbf{R}, 0)) = \mathrm{e}^{\mathrm{i}\mathbf{q}\cdot\mathbf{R}}\phi(\mathbf{y}),$$

for all lattice vectors $\mathbf{R}$.

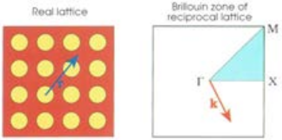

(picture taken from Joannopoulos et al., 1995)

Bloch waves

Periodicity of the geometry motivates to look for periodic solutions satisfying

$$\phi(\mathbf{y} + (\mathbf{R}, 0)) = \mathrm{e}^{\mathrm{i}\mathbf{q}\cdot\mathbf{R}}\phi(\mathbf{y}),$$

for all lattice vectors $\mathbf{R}$.

Equation (1) is unchanged if a reciprocal lattice vector $\mathbf{K}$ is added to $\mathbf{q}$.

Thus, given a solution $\phi(\mathbf{y}; \mathbf{q})$ then $\phi(\mathbf{y}; \mathbf{q} + \mathbf{K})$ is also a solution.

Consequently, it is sufficient to restrict attention to the *first Brillouin zone* $\{\mathbf{q} \mid \mathbb{R}\mathrm{e}\, q_1 \in (-\pi/R, \pi/R],\ \mathbb{R}\mathrm{e}\, q_2 \in (-\pi/S, \pi/S]\}$.

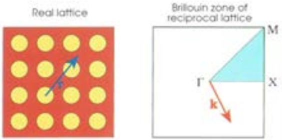

(picture taken from Joannopoulos et al., 1995)

Bloch waves

Periodicity of the geometry motivates to look for periodic solutions satisfying

$$\phi(\mathbf{y} + (\mathbf{R}, 0)) = \mathrm{e}^{\mathrm{i}\mathbf{q}\cdot\mathbf{R}}\phi(\mathbf{y}),$$

for all lattice vectors $\mathbf{R}$.

Only considering structures with constant depth dependence leads to solving the 2d Helmholtz equation subject to (1) as well as the conditions at the immersed surface ($\partial_n \phi = 0$ in what follows).
I.e. fixing two of k, q_1, and q_2 requires solving for the third.

Bloch waves

Periodicity of the geometry motivates to look for periodic solutions satisfying

$$\phi(\mathbf{y} + (\mathbf{R}, 0)) = \mathrm{e}^{\mathrm{i}\mathbf{q}\cdot\mathbf{R}}\phi(\mathbf{y}),$$

for all lattice vectors $\mathbf{R}$.

Only considering structures with constant depth dependence leads to solving the 2d Helmholtz equation subject to (1) as well as the conditions at the immersed surface ($\partial_n \phi = 0$ in what follows).
I.e. fixing two of k, q_1, and q_2 requires solving for the third.

A solution method for bottom-mounted circular cylinders solving for k for given (q_1, q_2) based on a variational formulation for the eigenvalue problem was given by McIver (2000).

We also implemented a finite element method for bodies of arbitrary cross-section as well as a method based on diffraction transfer operators (P. & Meylan, 2011).

Rainbow trapping

Idea

Use nearly periodic arrangement to slow down the wave to increase intensity locally.

Rainbow trapping

Idea

Use nearly periodic arrangement to slow down the wave to increase intensity locally.

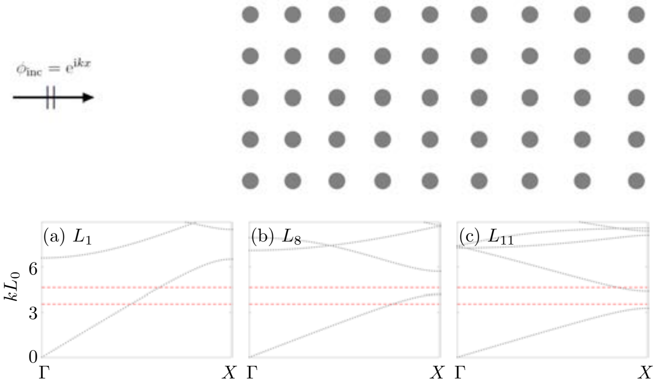

Rainbow trapping

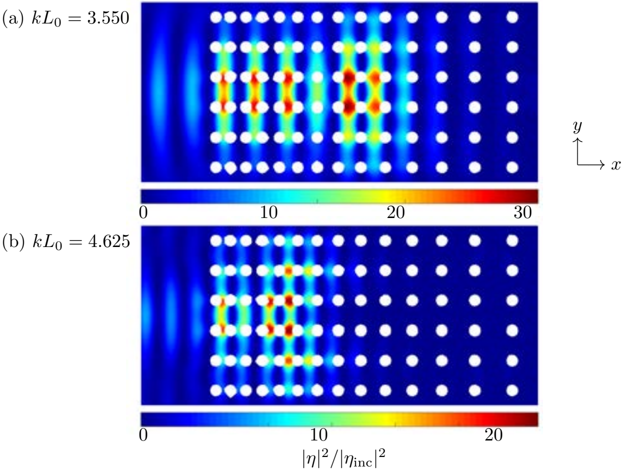

Ongoing research

Earlier this year at the wave flume of the University of Western Australia (Perth)

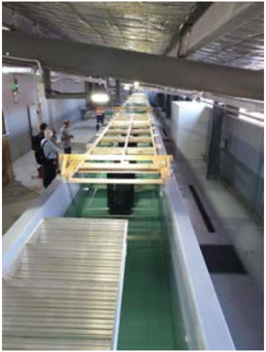

(joint work with Hugh Wolgamot and his group in Perth)

Ongoing research

Calculated and measured results in gaps 2 and 3.

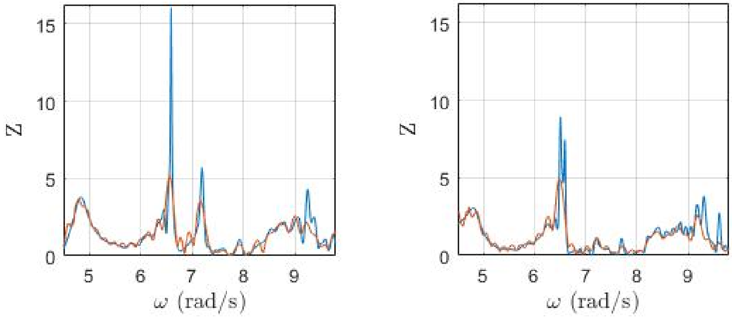

(joint work with Hugh Wolgamot and his group in Perth)

Chirp C-shapes

Here: Single (!) line of ten periodically spaced C-shaped bottom-mounted cylinders of increasing radius.

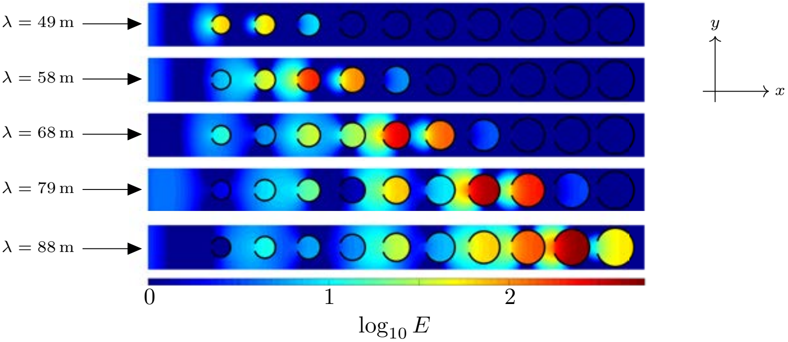

Chirp C-shapes

Here: Single (!) line of ten periodically spaced C-shaped bottom-mounted cylinders of increasing radius.

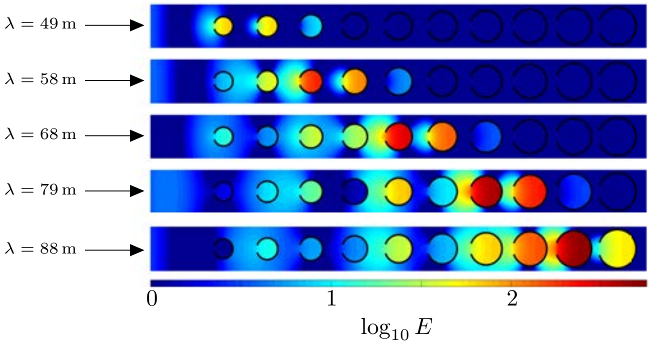

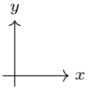

Rest of this talk: Consider two-dimensional arrays of C-shapes.

Bloch waves in a 2d grating

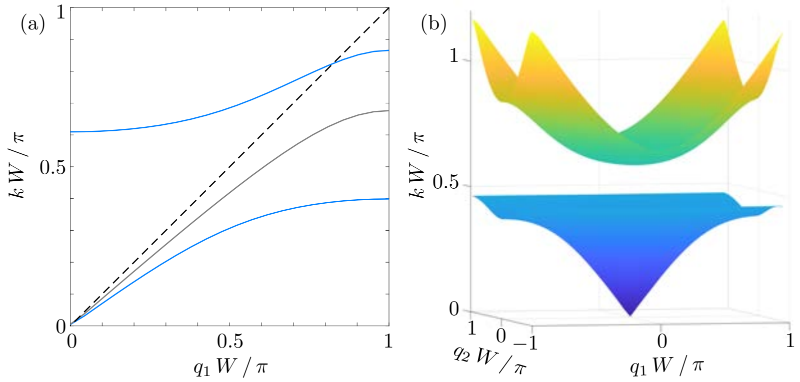

(a) Dispersion curves for $q_2 W = 0$, $a/W = 0.313$ and C-shaped resonator (solid blue curves) as well as closed circles (solid grey curve), with the light line overlaid (dashed black line).
(b) Dispersion surfaces for the C-shaped resonator.

Decompose geometry

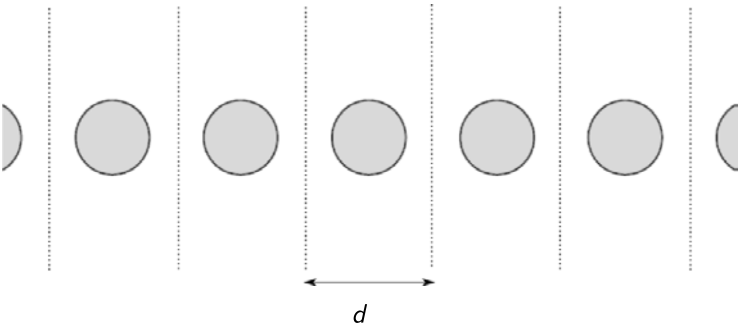

Stacks of single-line gratings

Define the scattering angles ψ_m by

$$\psi_m = \arcsin(\beta_m) \text{ where } \beta_m = \beta + \frac{2\pi m}{kW},$$

where ψ_0 is the angle between the direction of the incident wave and the x-axis. The wave field between columns m and $m+1$ is

$$\begin{aligned}\phi(x,y) &= \sum_{j=-\infty}^{\infty} a_j^{(m+)}\,\mathrm{e}^{\mathrm{i}\,k\,\{\beta_j\,y-\alpha_j\,(x-x_{m+})\}} + b_j^{(m+)}\,\mathrm{e}^{\mathrm{i}\,k\,\{\beta_j\,y+\alpha_j\,(x-x_{m+})\}},\\ &= \sum_{j=-\infty}^{\infty} b_j^{(m+1-)}\,\mathrm{e}^{\mathrm{i}\,k\,\{\beta_j\,y+\alpha_j\,(x-x_{m+1-})\}} + a_j^{(m+1-)}\,\mathrm{e}^{\mathrm{i}k\,\{\beta_j\,y-\alpha_j\,(x-x_{m+1-})\}},\end{aligned}$$

where $a_j^{(m\pm)}$ and $b_j^{(m\pm)}$, respectively, are the incoming and outgoing wave amplitudes, from the left $(-)$ and right $(+)$ of column m.

Stacks of single-line gratings

Truncation:

$$\begin{aligned}\phi(x,y) &\approx \mathrm{e}^{\mathrm{i}\,k\,\beta\,y}\left(\mathrm{e}^{-\mathrm{i}\,k\,\alpha\,(x-x_{m+})}\mathbf{a}_{m+} + \mathrm{e}^{\mathrm{i}\,k\,\alpha\,(x-x_{m+})}\mathbf{b}_{m+}\right),\\ &\approx \mathrm{e}^{\mathrm{i}\,k\,\beta\,y}\left(\mathrm{e}^{\mathrm{i}\,k\,\alpha\,(x-x_{m+1-})}\mathbf{a}_{m+1-} + \mathrm{e}^{-\mathrm{i}\,k\,\alpha\,(x-x_{m+1-})}\mathbf{b}_{m+1-}\right),\end{aligned}$$

where

$$\mathrm{e}^{\mathrm{i}\,k\,\beta\,y} = \mathrm{diag}\{\mathrm{e}^{\mathrm{i}\,k\,\beta_j\,y}\} \quad \text{and} \quad \mathrm{e}^{\pm\,\mathrm{i}\,k\,\alpha\,x} = \mathrm{diag}\{\mathrm{e}^{\pm\,\mathrm{i}\,k\,\alpha_j\,x}\},$$

$$\mathbf{a}_{m\pm} = \mathrm{vec}\{a_j^{m\pm}\} \quad \text{and} \quad \mathbf{b}_{m\pm} = \mathrm{vec}\{b_j^{m\pm}\}.$$

The transfer matrix $\mathcal{P}_m$ is the matrix that relates amplitudes on either side of column m, i.e.

$$\begin{pmatrix} \mathbf{b}_+ \\ \mathbf{a}_+ \end{pmatrix} = \mathcal{P}_m \begin{pmatrix} \mathbf{a}_- \\ \mathbf{b}_- \end{pmatrix}.$$

Transfer matrix of a single-line grating

The transfer matrix $\mathcal{P}_m$ is the matrix that relates amplitudes on either side of column m, i.e.

$$\begin{pmatrix} \mathbf{b}_+ \\ \mathbf{a}_+ \end{pmatrix} = \mathcal{P}_m \begin{pmatrix} \mathbf{a}_- \\ \mathbf{b}_- \end{pmatrix}.$$

The eigenvalues of the transfer matrix, $\{\mu \in \mathbb{C} : \mu \in (\mathcal{P}_m)\}$, make up the spectrum of the associated operator, and define the waves supported by the corresponding doubly-periodic array.

In particular, eigenvalues on the unit circle, $|\mu| = 1$, define Bloch wavenumbers on the bands via the relation $\mu = \exp(\mathrm{i}\, q_1\, W)$, with q_2 defined by the incident wave via $q_2 = k \sin \psi$.

Stacks of single-line gratings

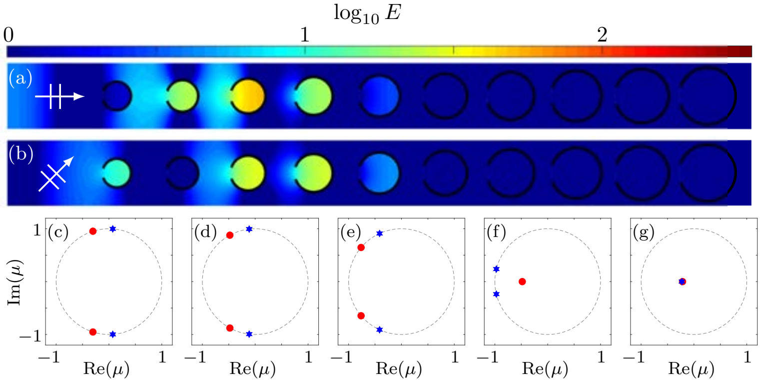

(c–g) Dominant eigenvalues of transfer matrices in complex plane, for head-on incidence (red bullets) and 45° incident wave (blue stars) operating over columns $n = 1, \ldots, 5$. Unit circles are overlaid (broken curves).

Stacks of single cylinders (or finite number)

Outside of the resonators, the total wave field, ϕ, is decomposed into fields propagating/decaying rightwards and leftwards on the left- and right-hand sides of the source via the integral representations

$$\phi(x, y) = \int_{\Gamma_\pm} A_{m\pm}(\chi)\,\varphi_{m\pm}(x, y : \chi)\,\mathrm{d}\chi + \int_{\Gamma_\mp} B_{m\pm}(\chi)\,\varphi_{m\pm}(x, y : \chi)\,\mathrm{d}\chi,$$

where

$$\varphi_\pm(x, y : \chi) = \mathrm{e}^{\mathrm{i}\,k\,\{(x - x_{m\pm})\,\cos\chi + y\,\sin\chi)\}}$$

is a plane wave travelling in direction χ and normalised to the left-hand side $(-)$ or right-hand side $(+)$ of the column. The integration contours are defined by

$$\Gamma_- = \{-\pi/2 + \mathrm{i}\gamma : \gamma \in \mathbb{R}_+\} \cup \{\gamma \in \mathbb{R} : -\pi/2 \le \gamma \le \pi/2\} \cup \{\pi/2 - \mathrm{i}\gamma : \gamma \in \mathbb{R}_+\},$$

and $\Gamma_+ = \Gamma_- + \pi$.

Stacks of single cylinders (or finite number)

$$\phi_{\mathrm{inc}}^{-} = \int_{-\frac{\pi}{2}+\mathrm{i}\infty}^{\frac{\pi}{2}-\mathrm{i}\infty} c_{-}(\chi)\varphi(\chi)\,\mathrm{d}\chi$$

$$\phi_{\mathrm{sca}}^{-} = \int_{\frac{\pi}{2}+\mathrm{i}\infty}^{\frac{3\pi}{2}-\mathrm{i}\infty} b_{-}(\chi)\varphi(\chi)\,\mathrm{d}\chi$$

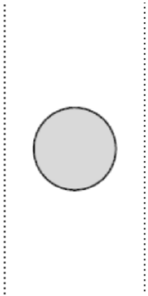

$$\phi_{\mathrm{sca}}^{+} = \int_{-\frac{\pi}{2}+\mathrm{i}\infty}^{\frac{\pi}{2}-\mathrm{i}\infty} b_{+}(\chi)\varphi(\chi)\,\mathrm{d}\chi$$

$$\phi_{\mathrm{inc}}^{+} = \int_{\frac{\pi}{2}+\mathrm{i}\infty}^{\frac{3\pi}{2}-\mathrm{i}\infty} c_{+}(\chi)\varphi(\chi)\,\mathrm{d}\chi$$

- $c_{\pm}(\chi)$ are incident amplitude functions
- $b_{\pm}(\chi)$ are scattered amplitude functions

Stacks of single cylinders (or finite number)

- Introduce scattering kernels R and T:

$$b_-(\chi) = \int_{-\frac{\pi}{2}+\mathrm{i}\infty}^{\frac{\pi}{2}-\mathrm{i}\infty} R(\chi|\psi)c_-(\psi)\,\mathrm{d}\psi + \int_{\frac{\pi}{2}+\mathrm{i}\infty}^{\frac{3\pi}{2}-\mathrm{i}\infty} T(\chi|\psi)c_+(\psi)\,\mathrm{d}\psi$$

$$b_+(\chi) = \int_{-\frac{\pi}{2}+\mathrm{i}\infty}^{\frac{\pi}{2}-\mathrm{i}\infty} T(\chi|\psi)c_-(\psi)\,\mathrm{d}\psi + \int_{\frac{\pi}{2}+\mathrm{i}\infty}^{\frac{3\pi}{2}-\mathrm{i}\infty} R(\chi|\psi)c_+(\psi)\,\mathrm{d}\psi$$

- Truncate complex branches and discretise χ-space. Gives array expressions:

$$\mathbf{b}_- = \mathcal{R}\mathbf{c}_- + \mathcal{T}\mathbf{c}_+ \quad \text{and} \quad \mathbf{b}_+ = \mathcal{T}\mathbf{c}_- + \mathcal{R}\mathbf{c}_+$$

- Associated <u>transfer matrix</u> (left-to-right map)

$$P = \begin{pmatrix} \mathcal{T} - \mathcal{R}\mathcal{T}^{-1}\mathcal{R} & \mathcal{R}\mathcal{T}^{-1} \\ -\mathcal{T}^{-1}\mathcal{R} & \mathcal{T}^{-1} \end{pmatrix}$$

Stacks of finite diffraction gratings

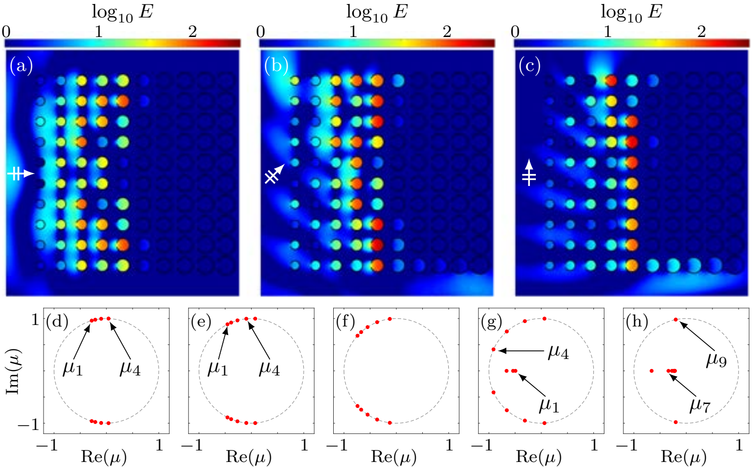

(d–h) Eigenvalues of transfer matrices corresponding to point spectrum of columns $m = 1, \ldots, 5$.

Summary

Summary

- Band diagrams are the key to understanding array-like structures. Computational approaches have been discussed.
- Understanding the spectrum of the transfer matrix is the key to tweaking array-like structures.
- Transfer-matrix formulations for different types of arrays were presented.
- Chirping of arrays can lead to high wave intensities (up factor 500 within linear theory!) at positions depending on the wave length. $\rightsquigarrow$ Rainbow trapping.